IJE TRANSACTIONS A: Basics Vol. 29, No. 7, (July 2016) 1005-1013

International Journal of Engineering

Journal Homepage: www.ije.ir

A Numerical Improvement in Analyzing the Dynamic Characteristics of an Electrostatically Actuated Micro-beam in Fluid Loading with Free Boundary Approach

D. Abdollahi*[a], K. Ivaz[a], R. Shabani[b]

[a] *Faculty of Mathematical Sciences, University of Tabriz, Tabriz, Iran*
[b] *Department of Mecanical Engineering, Urmia University, Urmia, Iran*

PAPER INFO

Paper history:
Received 18 April 2016
Received in revised form 23 May 2016
Accepted 02 June 2016

Keywords:
Free Boundary
Pull-in Voltage
Electrostatic Actuation
Added Mass
Micro-beam

ABSTRACT

In this paper, the dynamic response of a micro-beam immersed in a fluid with regard to the free boundary of the operating fluid is investigated. In the other words, in addition to the kinematic compatibility on the boundary between micro-beam and its surrounding fluid, equations of the potential functions are modeled considering the free boundaries. It is also assumed that the micro-beam is a movable electrode, and the electrostatic force is used for the actuation of the system. Galerkin's method is utilized to solve the governing equations of the fluid-structure system. By imposing a fixed voltage to the system, in addition to investigating the geometrical effects, fluid type and the dimensions of the cavity, the effect of the free boundaries on the transient response of the system is studied. It is shown that the coefficient of relative permittivity of operating fluid, the length of the micro-beam, and the relative position of it to the lower side of the cavity have significant impact on the instability of system voltage. It is further shown that assuming the free boundaries in the modeling of the system, which is closer to the physical reality of the issue, increases the pull-in voltage.

***doi**: 10.5829/idosi.ije.2016.29.07a.16*

1. INTRODUCTION

Micro-electro-mechanical systems (MEMS) have extensive applications in verity of devices such as micro-sensors, micro-mirrors, micro-switches, micro-pumps, microscopy and so fourth [1]. Nakhaei et al. [2] proposed a simple method for transverse vibrations of a cracked Euler-Bernoulli beam based on modeling crack as a stepped change in cross section of the beam. They showed that it is not necessary to model the crack as lumped flexibility model in order to fracture mechanics. Tadi et al. [3] derived the transverse vibration equation of cracked nano-beam based on modified couple stress theory. They calculated frequency parameters for different crack positions, different lengths of the beam, different crack properties, and some typical boundary conditions. Maroofi et al. [4] investigated thermoelastic damping (TED) of the longitudinal vibration of a homogeneous micro beam with both ends clamped. A Galerkin method has been used to analyze TED for the first mode of vibration of the micro beam.

In the design of the MEMS, the behavior of electrostatically actuated beams is affected by the beam deflections and the electric force. Therefore, these systems have an increasing interest over the past decades. One of the most important phenomena in MEMS is pull-in instability which happens when the actuated voltage exceeds the critical voltage. Abdalla et al. [5] presented a way to increase the pull-in voltage for an electrostatically actuated micro-beam by changing the micro-beam shape. They obtained optimal thickness and width designs for the micro-beam that maximize the pull-in voltage.

Lenci and Rega [6] studied a nonlinear electrically actuated micro-beam and its dynamic pull-in. They showed that how appropriate controlling superharmonics added to a reference harmonic

*Corresponding Author's Email: *d_abdollahi@tabrizu.ac.ir* (D. Abdollahi)

Please cite this article as: D. Abdollahi, K. Ivaz, R. Shabani, A Numerical Improvement in Analyzing the Dynamic Characteristics of an Electrostatically Actuated Micro-beam in Fluid Loading with Free Boundary Approach, International Journal of Engineering (IJE), TRANSACTIONS A: Basics Vol. 29, No. 7, (July 2016) 1005-1013

excitation succeed in shifting it towards higher excitation amplitudes. Hasanyan et al. [7] showed that the pull-in voltage can be regulated by varying volume fractions through the thickness of a functionally graded plate. Moghimi and Ahmadian [8] analyzed influences of intermolecular forces on the dynamic pull-in instability of electrostatically actuated beams. They developed a finite element model to discretize the governing equations using Newmark method. They showed that the attractive Casimir and van der Waals forces decrease the static pull-in deflection and pull-in voltage of micro-beam. Rezazadeh et al. [9] investigated the forced response of an electrostatically actuated micro-beam in an incompressible inviscid stationary fluid. Their results showed that increasing the fluid density and the aspect ratio of the beam increases the added mass and decreases the natural frequencies of the oscillating beam. Shabani et al. [10] presented the free vibrations of a cantilever micro-beam submerged in a bounded incompressible fluid domain. They investigated the effect of the fluid density and geometrical configuration on the natural frequencies of the coupled system using Galerkin's method. Askari and Tahani [11] studied the size-dependent dynamic pull-in of clamped-clamped micro-beams under mechanical shock. They derived the non-linear governing equation of motion utilizing Hamilton's principle. Golzar et al. [12] investigated the dynamic responses and pull-in instability of the electrostatically actuated micro-beam submerged in an incompressible viscous fluid cavity using equivalent squeeze film damping. They assumed all the boundaries were fixed in their model, but the beam-fluid interface was not fixed height throughout the length of the micro-beam along the x coordinate while vibrating (see [13] for more details). This fact could affect the domains of the potential functions in the mathematical model of the system.

In this study, we are interested in sketching an improved model based on the free boundary approach for the same system. In Section 2, we present the model of the system with free boundary approach. Section 3 verifies the method for various aspect and thickness ratios. In Section 4, the electrostatical instability of the system is analyzed with the proposed model to compare the obtained results with the pertinent work [12]. Finally, Section 5 completes this article with a brief conclusion.

2. MATHEMATICAL MODEL

Figure 1 illustrates a cantilever micro-beam of the length *l*, the thickness *h* and the width *b* in a cavity with the width *a* longer than *l* making it possible for two fluid domains to interact. It is assumed that the fluid is incompressible and inviscide. Therefore, the fluid movement induced by vibration of micro-cantilever could be described using velocity potential function in each fluid domain. However, oscillation of the micro-beam inside the chamber is subjected to a fluidic resistance which is caused by the fluid viscosity (μ). If the micro-beam length is much greater than its width, initial gap (g_0) is uniform and the vibration amplitude is much smaller than the initial gap. Consequently, an equivalent squeeze film damping is used in this paper [12, 16]. Taking into account the hydrodynamic pressures due to fluid oscillation in the lower and upper regions which are specified by P_1 and P_2, the governing equation of the motion for the actuated micro-beam by an electrostatic load of voltage V is written as [12]:

$$EI\frac{\partial^4\hat{w}}{\partial\hat{x}^4}+\mu b^3\left(\frac{1}{{g_1}^3}+\frac{1}{{g_2}^3}\right)\frac{\partial\hat{w}}{\partial\hat{t}}+\rho_B hb\frac{\partial^2\hat{w}}{\partial\hat{t}^2}=b\left(P_2-P_1\right)+\frac{k\,\varepsilon_0 b}{2}\left(\frac{V_{dc}}{g_1-\hat{w}\left(\hat{x},\hat{t}\right)}\right)^2 \quad (1)$$

where EI is the bending stiffness of the micro-beam, r_B is the mass per unit length and $w(x,t)$ describes the deflection at point x along the length of the micro-beam. The second term on the right side of Equation (1) denotes the electrostatic loading in the system. Parameters V_{dc}, k and $\varepsilon_0 = 8.85e-12\,F/m$ are the applied voltage, the dielectric coefficient of the gap medium and absolute dielectric constant of vacuum, respectively.

By the use of the following dimensionless variables:

$$x=\frac{\hat{x}}{a},\ w=\frac{\hat{w}}{g_1},\ y_1=\frac{\hat{y}_1}{g_1},\ y_2=\frac{\hat{y}_2}{g_2},\ t=\frac{\hat{t}}{t^*}, \quad (2)$$

Equation (1) is simplified as:

$$\frac{\partial^4 w}{\partial x^4}+z_1\left(1+\frac{{g_1}^3}{{g_2}^3}\right)\frac{\partial w}{\partial t}+\frac{\partial^2 w}{\partial t^2}=z_2\left(P_2-P_1\right)+z_3\left(\frac{V_{dc}}{1-w\left(x,t\right)}\right)^2 \quad (3)$$

in which:

$$t^*=\sqrt{\frac{\rho_B bha^4}{EI}},\ z_1=\frac{\mu b^3 a^4}{EI{g_1}^3 t^*},\ z_2=\frac{ba^4}{EIg_1},\ z_3=\frac{k\,\varepsilon_0 ba^4}{2EI{g_1}^3}. \quad (4)$$

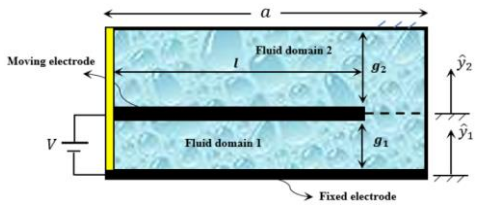

Figure 1. Electrostatically actuated micro-beam submerged in a fully contained cavity

Bernolli's equation and potential theory are employed to obtain the fluid pressures P_1 and P_2 as follow:

$$\begin{cases} P_1 = -\dfrac{\rho_f}{t^*}\dfrac{\partial \varphi_1(x, y_1, t)}{\partial t}\Big|_{y_1=1+w(x,t)} & (a) \\ P_2 = -\dfrac{\rho_f}{t^*}\dfrac{\partial \varphi_2(x, y_2, t)}{\partial t}\Big|_{y_2=w(x,t)}, & (b) \end{cases} \quad (5)$$

where φ_1 and φ_2 are the velocity potential functions of the fluids in the lower and upper regions of the micro-beam with the density ρ_f. These functions should be satisfied in the following Laplace equations with free boundary domains:

$$\nabla^2 \varphi_1(x, y_1, t) = 0, \quad \begin{cases} 0 < x < \dfrac{l}{a}, & 0 < y_1 < 1+w \\ \dfrac{l}{a} < x < l, & 0 < y_1 < 1 \end{cases} \quad (6)$$

$$\nabla^2 \varphi_2(x, y_2, t) = 0, \quad \begin{cases} 0 < x < \dfrac{l}{a}, & w < y_2 < 1 \\ \dfrac{l}{a} < x < l, & 0 < y_2 < 1 \end{cases} \quad (7)$$

in which the boundary conditions of φ_1 in the fluid domain 1 reads as follows:

$$\begin{cases} \dfrac{\partial \varphi_1}{\partial x}\Big|_{x=0,1} = 0, & 0 < y_1 < 1, \quad (a) \\ \dfrac{\partial \varphi_1}{\partial y_1}\Big|_{y_1=0} = 0, & 0 < x < 1, \quad (b) \\ \dfrac{1}{g_1}\dfrac{\partial \varphi_1}{\partial n_Q}\Big|_{y_1=1+w} = -\dfrac{g_1}{t^*}\dfrac{\partial w}{\partial t}, & 0 < x < \dfrac{l}{a}, \quad (c) \\ \dfrac{1}{g_1}\dfrac{\partial \varphi_1}{\partial y_1}\Big|_{y_1=1} = \dfrac{1}{g_2}\dfrac{\partial \varphi_2}{\partial y_2}\Big|_{y_2=0}, & \dfrac{l}{a} < x < 1, \quad (d) \end{cases} \quad (8)$$

In a similar way, φ_2 satisfies in the fluid domain 2 such as:

$$\begin{cases} \dfrac{\partial \varphi_2}{\partial x}\Big|_{x=0,1} = 0, & 0 < y_2 < 1, \quad (a) \\ \dfrac{\partial \varphi_2}{\partial y_2}\Big|_{y_2=0} = 0, & 0 < x < 1, \quad (b) \\ \dfrac{1}{g_2}\dfrac{\partial \varphi_2}{\partial n_Q}\Big|_{y_2=w} = -\dfrac{g_1}{t^*}\dfrac{\partial w}{\partial t}, & 0 < x < \dfrac{l}{a}, \quad (c) \\ \dfrac{1}{g_2}\dfrac{\partial \varphi_2}{\partial y_2}\Big|_{y_2=0} = \dfrac{1}{g_1}\dfrac{\partial \varphi_1}{\partial y_1}\Big|_{y_1=1}, & \dfrac{l}{a} < x < 1, \quad (d) \end{cases} \quad (9)$$

in which $\dfrac{\partial \varphi}{\partial n_Q}$ is the directional derivative of φ in the direction of the unit vector n_Q. Conditions (8c, 9c) state that the part of fluid immediately in contact with the lower and upper surfaces of the micro-beam has an equal velocity to the lateral velocity of the vibrating micro-beam. The method of separation of variables is applied to solve Equations (6) and (7) by imposing the impermeability conditions (8a, 8b) and (9a, 9b). Therefore, the following relations are obtained for the velocity potential functions φ_1 and φ_2 such as:

$$\begin{cases} \varphi_1(x, y_1, t) = \sum_{i=1}^{\infty} A_i(t)\cos(\lambda_i x)\cosh(\delta_i y_1), \\ \varphi_2(x, y_2, t) = \sum_{i=1}^{\infty} E_i(t)\cos(\lambda_i x) \\ \quad \times\left[\cosh(\gamma_i y_2) - \tanh(\gamma_i)\sinh(\gamma_i y_2)\right], \end{cases} \quad (10)$$

where the eigenvalues λ_i, δ_i and γ_i are equal to $i\pi$, $\dfrac{i\pi g_1}{a}$ and $\dfrac{i\pi g_2}{a}$, respectively. It should be noted that $A_i(t)$ and $E_i(t)$ are unknown modal amplitudes of fluid oscillation in Equation (10). The lateral motion of the micro-beam, $w(x,t)$ is formulated as a linear superposition of the free vibration modes in air as follows:

$$w(x,t) = \sum_{i=1}^{\infty} q_i(t)\psi_i(x), \quad (11)$$

in which $\psi_i(x)$ is the natural mode shapes of the micro-beam in air and the unknown generalized coordinates $q_i(t)$ should be estimated. The mode shapes are written as [14]:

$$\psi_i = \left(\sin(\beta_i l) + \sinh(\beta_i l)\right)\left(\sin(\beta_i x) - \sinh(\beta_i x)\right) - \left(\cos(\beta_i l) + \cosh(\beta_i l)\right)\left(\cos(\beta_i x) - \cosh(\beta_i x)\right) \quad (12)$$

where values of $\beta_i l$ must satisfy the transcendental equation:

$$\cosh(\beta_i l)\cos(\beta_i l) = -1. \quad (13)$$

The values $\beta_i l$ and the natural frequencies of the dry beam (ω_i) are satisfied in [13]:

$$\omega_i = (\lambda_i l)^2\sqrt{\frac{EI}{\rho_B l^4}}. \quad (14)$$

Inserting Equation (10) into the kinematic beam-fluid conditions (8c, 8d) and (9c, 9d) by using the orthogonality of $\cos(\lambda_j x)$ over $0<x<1$ yields the following relations:

$$\begin{cases} \frac{1}{g_1}\sum_{i=1}^{\infty} A_i(t)\delta_i\left[\Lambda_1(t)+\Lambda_2(t)\right]_{ji} = -\frac{g_1}{t^*}\sum_{i=1}^{\infty}\dot{q}_i(t)\alpha_{ji} \\ \qquad -\frac{1}{g_2}\sum_{i=1}^{\infty} E_i(t)\gamma_i\mu_{ji}\tan(\gamma_i), \qquad (a) \\ \frac{1}{g_2}\sum_{i=1}^{\infty} E_i(t)\gamma_i\left[\Lambda_3(t)+\Lambda_4(t)\right]_{ji} = -\frac{g_1}{t^*}\sum_{i=1}^{\infty}\dot{q}_i(t)\alpha_{ji} \\ \qquad +\frac{1}{g_1}\sum_{i=1}^{\infty} A_i(t)\delta_i\mu_{ji}\sinh(\delta_i), \qquad (b) \end{cases} \tag{15}$$

where coefficients μ_{ji}, α_{ji} and $\Lambda_i(t)$ $(1\le i\le 4)$ are defined as:

$$\begin{cases} \alpha_{ji} = \int_0^{\frac{l}{a}} \cos(\lambda_j x)\psi_i(x)dx, \\ \mu_{ji} = \int_0^{\frac{l}{a}} \cos(\lambda_i x)\cos(\lambda_j x)dx, \\ \Lambda_1(t) = \int_0^1 \cos(\lambda_i x)\sinh\left[\delta_i(1+w)\right]\frac{\cos(\lambda_j x)}{\sqrt{1+w_x^2}}dx, \\ \Lambda_2(t) = \int_0^1 \sin(\lambda_i x)\cosh\left[\delta_i(1+w(x,t)\right] \\ \qquad \times\frac{w_x(x,t)}{\sqrt{1+w_x^2(x,t)}}\cos(\lambda_j x)dx, \\ \Lambda_3(t) = \int_0^1 \cos(\lambda_i x)\left[\sinh(\gamma_i w(x,t)) - \tanh(\gamma_i)\right. \\ \qquad \left.\times\cosh(\gamma_i w(x,t))\right]\frac{\cos(\lambda_j x)}{\sqrt{1+w_x^2(x,t)}}dx, \\ \Lambda_4(t) = \int_0^1 \sin(\lambda_i x)\left[\cosh(\gamma_i w(x,t)) - \tanh(\gamma_i)\right. \\ \qquad \left.\times\sinh(\gamma_i w(x,t))\right]\frac{w_x(x,t)}{\sqrt{1+w_x^2(x,t)}}\cos(\lambda_j x)dx, \end{cases} \tag{16}$$

Substituting Equation (10) into Equation (5) and inserting the outcome into Equation (3) by using Equation (11) gives equation of the motion for the micro-beam as follows:

$$\begin{aligned} &\sum_{i=1}^{\infty} q_i(t)\psi_i^{(4)}(x) + z_1\left(1+\frac{g_1^3}{g_2^3}\right)\sum_{i=1}^{\infty}\dot{q}_i(t)\psi_i(x) \\ &\quad +\sum_{i=1}^{\infty}\ddot{q}_i(t)\psi_i(x) = \frac{z_2\rho_f}{t^*}\left[\sum_{i=1}^{\infty}\dot{A}_i(t)\cos(\lambda_i x)\right. \\ &\quad \times\cosh\left[\delta_i(1+w(x,t)\right] - \sum_{i=1}^{\infty}\dot{E}_i(t)\cos(\lambda_i x) \\ &\quad \left.\times\left(\cosh\left[\gamma_i w\right] - \tanh(\gamma_i)\sinh\left[\gamma_i w\right]\right)\right] + \frac{z_3 V_{dc}^2}{(1-w)^2}. \end{aligned} \tag{17}$$

Making use of the orthogonality of the beam mode shapes in Equation (17), the following equation is derived:

$$\begin{aligned} &\left[\int_0^{\frac{l}{a}}\psi_j^{(4)}(x)\psi_j(x)dx\right]q_j(t) + z_1\left(1+\frac{g_1^3}{g_2^3}\right) \\ &\quad \times\left[\int_0^{\frac{l}{a}}\psi_j^2(x)dx\right]\dot{q}_j(t) + \left[\int_0^{\frac{l}{a}}\psi_j^2(x)dx\right]\ddot{q}_j(t) \\ &\quad = \frac{z_2\rho_f}{t^*}\left[\sum_{i=1}^{\infty}\dot{A}_i(t)\int_0^{\frac{l}{a}}\cos(\lambda_i x)\right. \\ &\qquad \left.\times\cosh\left[\delta_i(1+\mathrm{w(x,t)})\right]\psi_j(x)dx\right. \\ &\quad -\sum_{i=1}^{\infty}\dot{E}_i(t)\int_0^{\frac{l}{a}}\cos(\lambda_i x)\left[\cosh\left[\gamma_i w(x,t)\right]\right. \\ &\qquad \left.\left.-\tanh(\gamma_i)\sinh\left[\gamma_i w(x,t)\right]\right)\psi_j(x)dx\right] \\ &\qquad +z_3\int_0^{\frac{l}{a}}\left(\frac{V_{dc}}{1-w(x,t)}\right)^2\psi_j(x)\,\mathrm{dx}. \end{aligned} \tag{18}$$

Now, the micro-beam and fluid vibration modes are truncated to *n* and *m* modes, respectively. Therefore, the finite set of matrix equations is derived by rewriting Equation s (15) and (18) as follows:

$$[L]\{A\} = [D]\{\dot{q}\} - [G]\{E\}, \tag{19}$$

$$-[R]\{E\} = [D]\{\dot{q}\} + [N]\{A\}, \tag{20}$$

$$[K]\{q\} + [S]\{\dot{q}\} + [M]\{\ddot{q}\} = [C]\{\dot{A}\} - [J]\{\dot{E}\} + F, \tag{21}$$

where the elements of the coefficient matrices are calculated by the following relations:

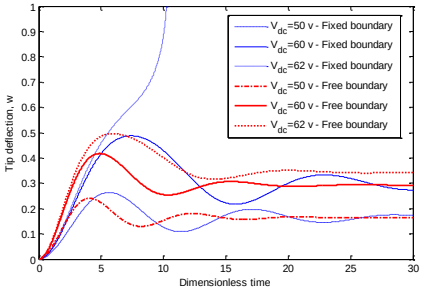

Figure 2. Dimensionless time history for the micro-beam in *CCl*4

$$\begin{cases} L_{ij} = \frac{1}{g_1}\delta_j \left[\Lambda_1(t)+\Lambda_2(t)\right]_{ij}, \\ D_{ij} = -\frac{g_1}{t^*}\alpha_{ij},\ G_{ij} = \frac{1}{g_2}\gamma_j \mu_{ij} \tanh(\gamma_j), \\ \mathrm{R}_{ij} = \frac{1}{g_2}\gamma_j \left[\Lambda_3(t)+\Lambda_4(t)\right]_{ij}, \\ N_{ij} = \frac{1}{g_1}\delta_j \mu_{ij} \sinh\left(\delta_j\right),\ K_{ii} = \int_0^{\frac{l}{a}} \psi_i^{(4)}(x)\psi_i(x)dx, \\ M_{ii} = \int_0^{\frac{l}{a}} \psi_i^2(x)\,\mathrm{dx}, S_{ij} = z_1\left(1+\frac{g_1^3}{g_2^3}\right)\int_0^{\frac{l}{a}} \psi_i^2(x)dx, \\ C_{ij} = \frac{z_2\rho_f}{t^*}\int_0^{\frac{l}{a}} \cos(\lambda_i x) \\ \qquad \times\cosh\left[\delta_j(1+w(x,t))\right]\psi_i(x)dx, \\ J_{ij} = -\frac{z_2\rho_f}{t^*}\int_0^{\frac{l}{a}} \cos(\lambda_j x)\left(\cosh\left[\gamma_j w(x,t)\right]\right. \\ \qquad \left.-\tanh(\gamma_j)\sinh\left[\gamma_j w(x,t)\right]\psi_i(x)\right)dx, \\ F = z_3\int_0^{\frac{l}{a}}\left(\frac{V_{dc}}{1-w(x,t)}\right)^2 \psi_j(x)dx. \end{cases} \quad (22)$$

By substituting the generalized fluid coordinates A and E from Equations (19) and (20) into Equation (21), the following system of *n* unknowns and equations is obtained for the generalized coordinates of the micro-beam :

$$\left(\left[M\right]+\left[M_1\right]+\left[M_2\right]\right)\{\ddot{q}\}+\left[S\right]\{\dot{q}\}\left[K\right]\{q\}=F. \quad (23)$$

where M_1 and M_2 are the added mass of the fluid domains 1 and 2, respectively. These two-part added mass are the result of the presence of the fluid around the micro-beam that are defined as follows:

$$\begin{cases} M_1 = \left[CL^{-1}D\right]+\left[CL^{-1}G\right] \\ \qquad \times\left(\left[R\right]+\left[NL^{-1}G\right]\right)^{-1}\left(\left[D\right]+\left[NL^{-1}D\right]\right), \\ M_2 = -\left[J\right]\left(\left[R\right]+\left[NL^{-1}G\right]\right)^{-1}\left(\left[D\right]+\left[NL^{-1}D\right]\right). \end{cases} \quad (24)$$

The solution would be estimated using Newmark method for different step DC voltages.

3. VERIFICATION OF THE METHOD

In order to validate the proposed method, Table 1 shows the comparison of fundamental frequencies in water ($\rho_f = 1000 kg/m^3$) for various aspect ratios $\left(l/b\right)$ and thickness ratios $\left(h/b\right)$ with previous studies.

This is done by omitting the nonlinear forcing term and fluid damping. The obtained results are in agreement with the experimental results of Lindholm et al. [15], the analytical results of Liang et al. [16], Golzar et al. [12] and our recent work [13]. Furthermore, percentage of the errors between the results obtained by the free boundary method and experimental results are included in Table 1.

4. NUMERICAL RESULTS

The natural frequencies and mode shapes of the micro-beam submerged in water are compared with both fixed and free boundary approaches. The physical properties and the values of the used parameters are listed in Table 2 and 3.

It should be mentioned that the width of the micro-beam meets $b \geq 5h$. Consequently, the micro-beam strain conditions should be taken into consideration. Therefore, E is replaced by $E/(1-\nu^2)$, where ν is Poisson's ratio. Figure 2 shows that the response of the micro-beam varies for different input voltages in CCl_4.

TABLE 1. Comparison of fundamental frequencies in water

Aspect ratio, *l*/*b*	**5**	**3**	**2**	**1**
Thickness ratio, *h*/*b*	**0.125**	**0.061**	**0.061**	**0.024**
ω_1 (Hz)	15.63	18.30	42.30	51.93
Analytical (Liang et al. [16])	14.60	17.80	40.30	51.40
Experimental (Lindholm et al. [15])	15.62	18.82	46.80	57.90
Fixed boundary (Golzar et al. [12])	15.62	18.82	46.80	57.90
Analytical (Abdollahi et al. [13])	13.09	17.89	40.24	59.33
Proposed method (Error percentage)	15.16 (3%)	18.27 (3%)	45.32 (3.25%)	54.38 (6.47%)

TABLE 2. The data used in the calculations

Parameter	Value
Micro-beam width, b	25 μm
Micro-beam length, l	250 μm
Micro-beam thickness, h	3 μm
Container length, a	350 μm
Liquid depth of domain 1, g_1	4 μm
Liquid depth of domain 2, g_2	10 μm
Young's modulus, E	169 Gpa
Micro-beam mass, ρ_B	2330 kg/m^3
Poisson's ratio, ν	0.06
Number of fluid oscillation modes, m	5
Number of beam vibration modes, n	3

TABLE 3. The data of the fluid used in the calculations

Fluid	kg/m^3 ρ_f	Dielectric coefficient, K	Viscosity, μ $(Pa.s)$
Acetone	785	20.70	3.08e-4
Carbon tetrachloride	1590	2.20	8.79e-4
Water	997	80	8.59e-4

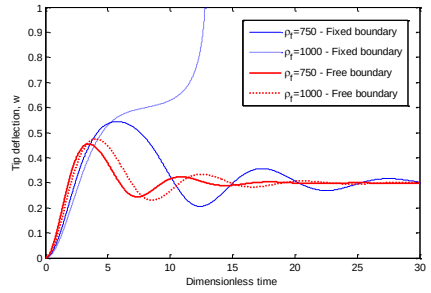

(a)

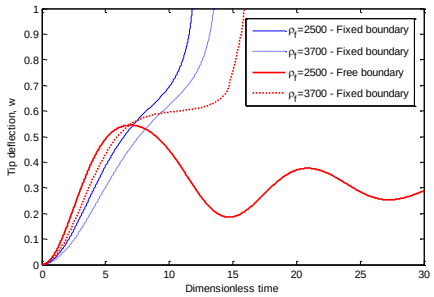

(b)

Figure 3. Effect of density on the dynamic response of micro-beam $(\mu = 500e-6\,Pa.s,\ V = 20v,\ k = 20)$

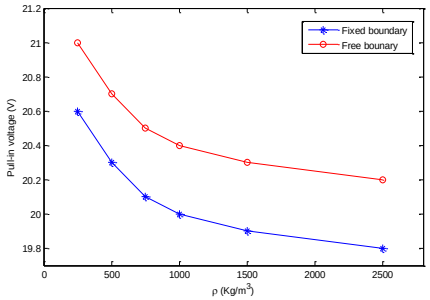

Figure 4. Effect of density on the pull-in voltage $(\mu = 500e-6\,Pa.s,\ k = 20)$

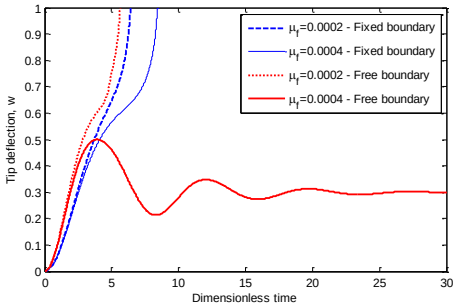

Figure 5. Effect of viscosity on the pull-in voltage $(V = 20v,\ k = 20,\ \rho = 900e-6\,Pa.s)$

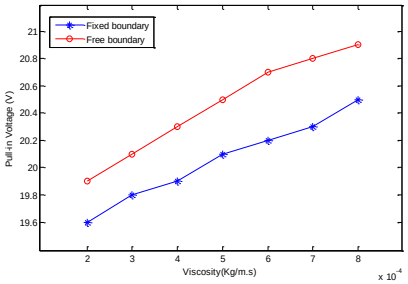

Figure 6. Effect of viscosity on the dynamic response of micro-beam $(\rho = 900e-6\,Pa.s,\ k = 20)$

It is seen that as input voltage increases the amplitude of response increases with both fixed and free boundary states. But, the growth of the amplitude of response obtained with the proposed approach is slower than what presented with fixed boundary state by Golzar et al. [12]. Figure 3 presents that for higher fluid densities the response frequency decreases and the micro-beam is less resilient against the input voltage. In addition, the dynamic pull-in instability is varied from $\rho_f = 1000$ to $\rho_f = 2500$ with the proposed method.

Figure 4 illustrates the decrease of the values of the pull-in voltage for higher fluid densities with both approaches. Nevertheless, the pull-in voltage increases

about 2% in comparision with the fixed boundary method [12]. Figure 5 shows the effect of viscosity in the pull-in voltages. It is demonstrated that higher input voltages are required to cause pull-in phenomenon in the system. But, Figure 6 reveals that the area of pull-in voltage is more than what has been obtained with fixed boundary approach. It means that the system becomes more stable by free boundary approach.

Figure 7 proves that the electrostatic instability happens at great values of the dielectric constant. It is interesting that the system is stable for k = 21 with free boundary approach. Figure 8 studies the effect of gap height on the dynamic response of the micro-beam by altering the vertical position of it $(g_1 + g_2 = 14\mu m)$.

It shows that pull-in voltage decreases in the lower position of the micro-beam. Figure 9 presents that increasing the length of the micro-beam decreases the pull-in voltage of the system with both approaches.

Figure 10 depicts the response of the micro-beam submerged in water, acetone and carbon tetrachloride with fixed and free boundary states. It is clear that the amplitude of response is lower than what obtained by Golzar et al. [12] for three types of liquids.The effect of fluid oscillation modes on the pull-in voltage is shown in Figure 11. It is seen that as the number of fluid modes increases, the rate of convergence grows as well.

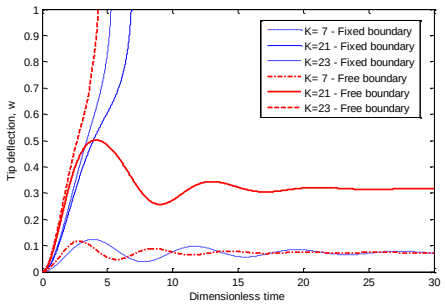

(a)

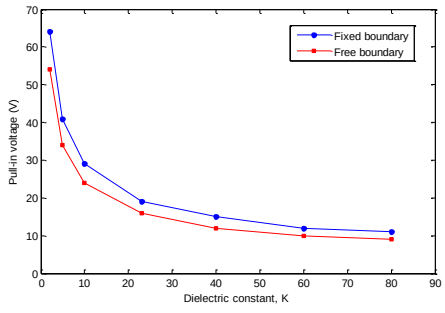

(b)

Figure 7. Effect of dielectric constant on the dynamic response of micro-beam $(\rho = 900e-6\,Pa.s,\ k = 20,\ \mu = 500e-6\,Pa.s)$

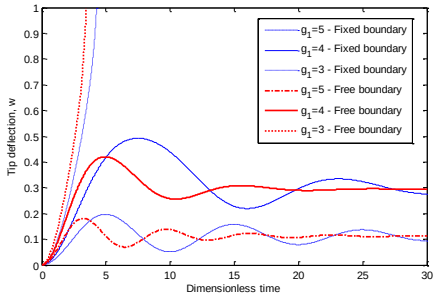

(a)

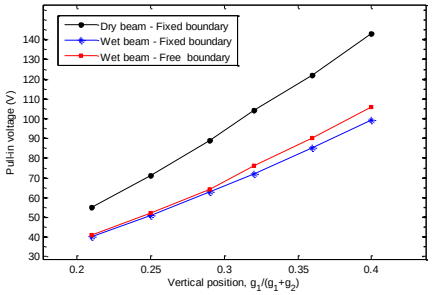

(b)

Figure 8. Effect of gap height on the dynamic response of micro-beam CCl_4, (a) time history and (b) pull-in voltage

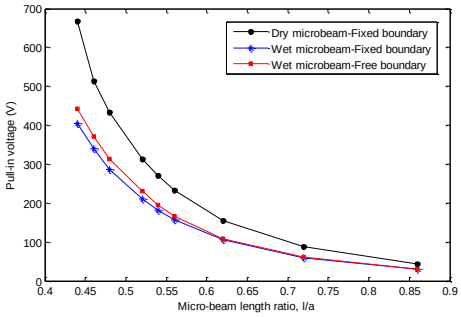

Figure 9. Pull-in voltage for different micro-beam lengths, (CCl_4)

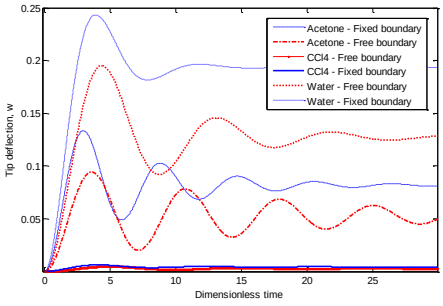

Figure 10. Dynamic response of the micro-beam for three working fluids

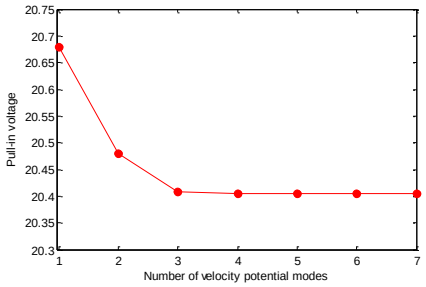

Figure 11. Convergency of the method ($\rho = 900e-6\,Pa.s$, $\mu = 500e-6\,Pa.s$, $k = 20$)

5. CONCLUDING REMARKS

The dynamic response of an electrostatically actuated micro-beam submerged in an incompressible viscous fluid cavity was analyzed. Significant transformations occurred at the conditions of instability of micro-beams, and as a consequence, the boundaries of the fluid surrounding the micro-beam underwent large variations. In this study, in addition to the conditions of kinematic compatibility of the fluid-structure, the equations governing the fluid have been modeled by assuming free boundary approach and Galerkin's semi-analytical method was utilized to solve the coupled equations. It was shown that assuming the free boundaries of the fluid, which is also closer to the physical reality, increases the stability of the system.

It was further shown that the coefficient of the fluid permittivity and the relative position of the micro-beam to the fixed electrode would change the amplitude of the pull-in voltage. The effects of the density and viscosity of the fluid and the length of the micro-beam on the dynamic response of the system were analyzed. Finally, it was concluded that assumption of the free boundaries for the fluid (in the equations of the potential functions) can be used for improving the manufacturing technology and design.

6. REFERENCE

1. Amiri, A., Fakhari, S., Pournaki, I., Rezazadeh, G. and Shabani, R., "Vibration analysis of circular magneto-electro-elastic nano-plates based on eringen's nonlocal theory", ***International Journal of Engineering-Transactions C: Aspects***, Vol. 28, No. 12, (2015), 1808-1817.
2. Nakhaei, A., Dardel, M., Ghasemi, M. and Pashaei, M., "A simple method for modeling open cracked beam", ***International Journal of Engineering-Transactions B: Applications***, Vol. 28, No. 2, (2014), 321-329.
3. Beni, Y. T., Jafaria, A. and Razavi, H., "Size effect on free transverse vibration of cracked nano-beams using couple stress theory", ***International Journal of Engineering-Transactions B: Applications***, Vol. 28, No. 2, (2014), 296-304.
4. Maroofi, M., Najafi, S., Shabani, R. and Rezazadeh, G., "Investigation of thermoelastic damping in the longitudinal vibration of a micro beam", ***International Journal of Engineering-Transactions B: Applications***, Vol. 28, No. 2, (2014), 314-320.
5. Abdalla, M. M., Reddy, C. K., Faris, W. F. and Gürdal, Z., "Optimal design of an electrostatically actuated microbeam for maximum pull-in voltage", ***Computers & Structures***, Vol. 83, No. 15, (2005), 1320-1329.
6. Lenci, S. and Rega, G., "Control of pull-in dynamics in a nonlinear thermoelastic electrically actuated microbeam", ***Journal of Micromechanics and Microengineering***, Vol. 16, No. 2, (2006).
7. Hasanyan, D., Batra, R. and Harutyunyan, S., "Pull-in instabilities in functionally graded microthermoelectromechanical systems", ***Journal of Thermal Stresses***, Vol. 31, No. 10, (2008), 1006-1021.
8. Zand, M. M. and Ahmadian, M., "Dynamic pull-in instability of electrostatically actuated beams incorporating casimir and van der waals forces", ***Proceedings of the Institution of Mechanical Engineers, Part C: Journal of Mechanical Engineering Science***, Vol. 224, No. 9, (2010), 2037-2047.
9. Rezazadeh, G., Fathalilou, M., Shabani, R., Tarverdilou, S. and Talebian, S., "Dynamic characteristics and forced response of an electrostatically-actuated microbeam subjected to fluid loading", ***Microsystem Technologies***, Vol. 15, No. 9, (2009), 1355-1363.
10. Shabani, R., Hatami, H., Golzar, F., Tariverdilo, S. and Rezazadeh, G., "Coupled vibration of a cantilever micro-beam submerged in a bounded incompressible fluid domain", ***Acta Mechanica***, Vol. 224, No. 4, (2013), 841-850.
11. Askari, A. R. and Tahani, M., "Size-dependent dynamic pull-in analysis of beam-type mems under mechanical shock based on the modified couple stress theory", ***Applied Mathematical Modelling***, Vol. 39, No. 2, (2015), 934-946.
12. Golzar, F. G., Shabani, R., Hatami, H. and Rezazadeh, G., "Dynamic response of an electrostatically actuated micro-beam in an incompressible viscous fluid cavity", ***Journal of Microelectromechanical Systems,*** Vol. 23, No. 3, (2014), 555-562.
13. Abdollahi, D., Ahdiaghdam, S., Ivaz, K. and Shabani, R., "A theoretical study for the vibration of a cantilever microbeam as a free boundary problem", ***Applied Mathematical Modelling***, Vol. 40, No. 3, (2016), 1836-1849.
14. Hosaka, H., Itao, K. and Kuroda, S., "Damping characteristics of beam-shaped micro-oscillators", ***Sensors and Actuators A: Physical***, Vol. 49, No. 1, (1995), 87-95.
15. Lindholm, U. S., Kana, D. D., Chu, W.-H. and Abramson, H. N., "Elastic vibration characteristics of cantilever plates in water", (1962), DTIC Document.
16. Liang, C.-C., Liao, C.-C., Tai, Y.-S. and Lai, W.-H., "The free vibration analysis of submerged cantilever plates", ***Ocean Engineering***, Vol. 28, No. 9, (2001), 1225-1245.

A Numerical Improvement in Analyzing the Dynamic Characteristics of an Electrostatically Actuated Micro-beam in Fluid Loading with Free Boundary Approach

D. Abdollahi[a], K. Ivaz[a], R. Shabani[b]

[a] *Faculty of Mathematical Sciences, University of Tabriz, Tabriz, Iran*
[b] *Department of Mecanical Engineering, Urmia University, Urmia, Iran*

P A P E R I N F O

Paper history:
Received 18 April 2016
Received in revised form 23 May 2016
Accepted 02 June 2016

Keywords:
Free Boundary
Pull-in Voltage
Electrostatic Actuation
Added Mass
Micro-beam

چکیده

در این مقاله پاسخ دینامیکی میکرو–تیر غوطه‌ور در سیال با در نظر گرفتن مرز آزاد سیال عمل کننده مورد بررسی قرار گرفته است. به عبارت دیگر علاوه بر سازگاری سینماتیکی در مرز بین میکرو–تیر و سیال اطراف آن، معادلات مربوط به تابع پتانسیل سیال با در نظر گرفتن مرزهای متحرک مدل‌سازی شده‌اند. همچنین فرض شده که میکرو–تیر مورد نظر به عنوان الکترود متحرک بوده و از نیروی الکترواستاتیک به عنوان تحریک سیستم استفاده شده است. معادلات حاکم بر سیستم سازه–سیال با استفاده از روش گالرکین حل شده‌اند. با اعمال ولتاژهای ثابت به سیستم، علاوه بر بررسی اثرات هندسی، نوع سیال و ابعاد محفظه، اثر مرزهای آزاد سیال بر پاسخ‌گذرای سیستم مورد بررسی قرار گرفته است. نشان داده شده است که ضریب گذردهی نسبی سیال عمل کننده، طول میکرو–تیر و موقعیت نسبی میکرو–تیر نسبت به کف محفظه تاثیر قابل توجهی در ولتاژ ناپایداری سیستم دارند. همچنین فرض مرزهای آزاد در مدل‌سازی سیستم که به واقعیت فیزیک مسأله نزدیک‌تر می‌باشد، باعث افزایش ولتاژ ناپایداری سیستم می‌گردد.

***doi**: 10.5829/idosi.ije.2016.29.07a.16*